

## Supplementary information

### Thermal degradation of lead halide perovskite surfaces

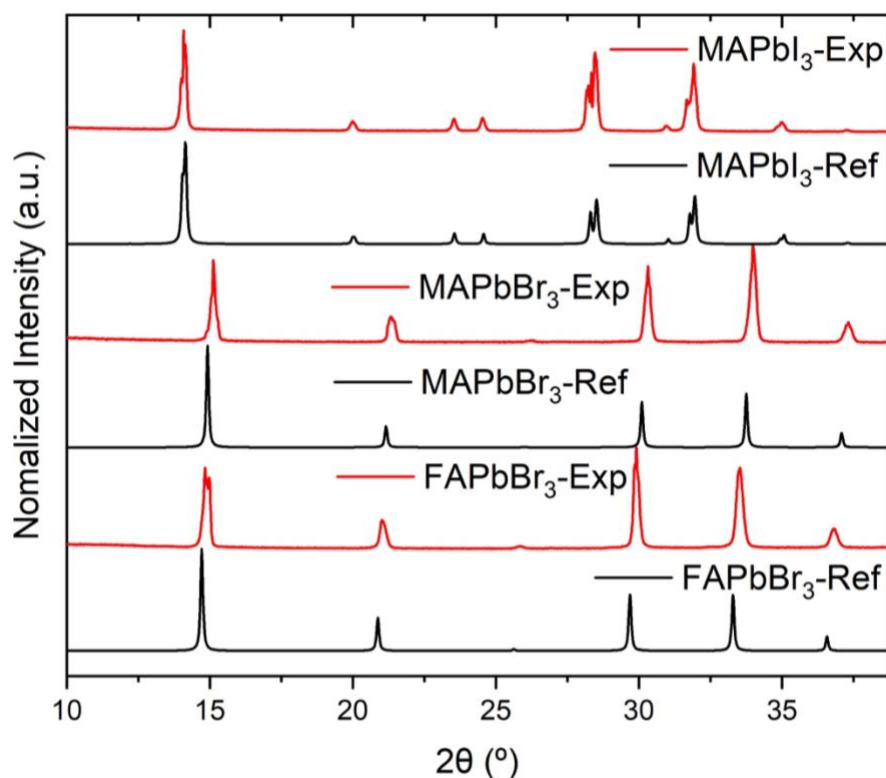
Birgit Kammlander, Sebastian Svanström, Danilo Kühn, Fredrik Johansson, Swarnshikha Sinha, Håkan Rensmo, Alberto García Fernández, Ute B. Cappel\*

## Experimental

### Synthesis of single crystals and X-ray diffraction characterization

Three different hybrid organic-inorganic single crystal compositions were studied: Methylammonium lead iodide ( $\text{CH}_3\text{NH}_3\text{PbI}_3$ , MAPbI<sub>3</sub>), methylammonium lead bromide ( $\text{CH}_3\text{NH}_3\text{PbBr}_3$ , MAPbBr<sub>3</sub>) and formamidinium lead bromide ( $\text{CH}_2(\text{NH}_2)_2$ , FAPbBr<sub>3</sub>). All single crystals were grown following an inverse temperature crystallization (ITC) methodology. All starting materials were used without any modification. Methylammonium iodide ( $\text{CH}_3\text{NH}_3\text{I}$ , MAI), methylammonium bromide ( $\text{CH}_3\text{NH}_3\text{Br}$ , MABr) and formamidinium bromide ( $\text{CH}(\text{NH}_2)_2\text{Br}$ , FABr) were purchased at Sigma-Aldrich and  $\text{PbI}_2$  and  $\text{PbBr}_2$  at TCI. Three 1M solutions with 1:1 ratio of MAI:PbI<sub>2</sub> in in gamma-butyrolactone (GBL) for MAPbI<sub>3</sub>, MABr:PbBr<sub>2</sub> (for MAPbBr<sub>3</sub>) and FABr:PbBr<sub>2</sub> (for FAPbBr<sub>3</sub>) both in dimethylformamide (DMF) were prepared at room temperature in ambient conditions. After all the precursors were completely dissolved the solution was filtered through a 0.45  $\mu\text{m}$  PTFE filter and heated up to 100 °C for MAPbI<sub>3</sub> and 80 °C for MAPbBr<sub>3</sub> and FAPbBr<sub>3</sub> single crystals. Single crystals of about 0.5 cm of diameter were obtained.

All selected single crystals were kept under nitrogen conditions and transported to BESSY II to be mounted, cleaved and measured. The rest of single crystals from the same batch were grounded using a pestle and mortar and powder X-ray diffraction measurements were carried out to check the purity of the phase. As can be seen in Figure S1 all samples present a single-phase material showing a perfect agreement between the experimental data and the profile obtained by single crystal XRD.



S 1: Experimental PXRD pattern of the polycrystalline powder of grounded single crystals (Red) of FAPbBr<sub>3</sub>, MAPbBr<sub>3</sub> and MAPbI<sub>3</sub> compared with the profile obtained from their single crystal structures at room temperature (black).

## Experimental set-up beamline

The selected crystals were mounted on the sample plates using EPO-TEK H20E two component epoxy. The epoxy was cured at 100 °C for 1 h in ambient air conditions. To ensure a clean surface, the crystals were cleaved under a pressure of around  $10^{-7}$  mbar and transferred to the main chamber in which they were characterized below  $2.3 \times 10^{-9}$  mbar. After that and without any movement, the crystals were heated in the main analysis chamber at a rate of 25 °C/h using a PID controlled resistive heater. The temperature was measured with a K-type thermocouple which is attached to the spring that clamps the sample plate to the manipulator. The temperature setting was PID controlled.

Photoelectron spectroscopy (PES) measurements of all single crystals were performed at the COESCA endstation1, UE-52 PGM beamline at the synchrotron facility BESSY II in Berlin, Germany. The single bunch X-rays were generated using a UE-52 undulator with pulse picking by resonant excitation (PPRE)2 during hybrid bunch operation and the energies selected using the beamline's plane grating monochromator beamline. The exit slit was fixed at 100  $\mu\text{m}$  for all core levels to control the X-ray intensity. Photoelectrons were detected using a Scienta ArTOF2-EW (56° angular acceptance) spectrometer (Angle-Resolved Time-Of-Flight spectrometer). Beam damage on the perovskites was avoided by using a low X-ray flux enabled by the high transmission of the ArTOF2 spectrometer. The pressure was below  $2.3 \times 10^{-9}$  mbar before starting the measurements but increased during the heating due to degassing processes of the single crystals up to  $5.5 \times 10^{-7}$  mbar. All measurements were done in fixed mode using a photon energy of 600 eV. The (kinetic) center energies were set as follows: I 4d: 545 eV; Br 3d: 526 eV; Pb 4f: 455 eV; C 1s: 308 eV; N 1s: 195/194 eV (FA/MA-based crystal).

All spectra were energy calibrated using Au 4f<sub>7/2</sub> core level (84.0 eV) as a reference and intensity normalized to the Pb 4f core level of each material. Data analysis of all core level spectra was performed by fits using a pseudo-Voigt function<sup>3</sup> with a polynomial or Shirley background<sup>4</sup>, depending on the shape of each core level background. All core levels positions agree with our previous work in which we present a detailed surface characterization of different perovskite single crystals.<sup>5</sup>

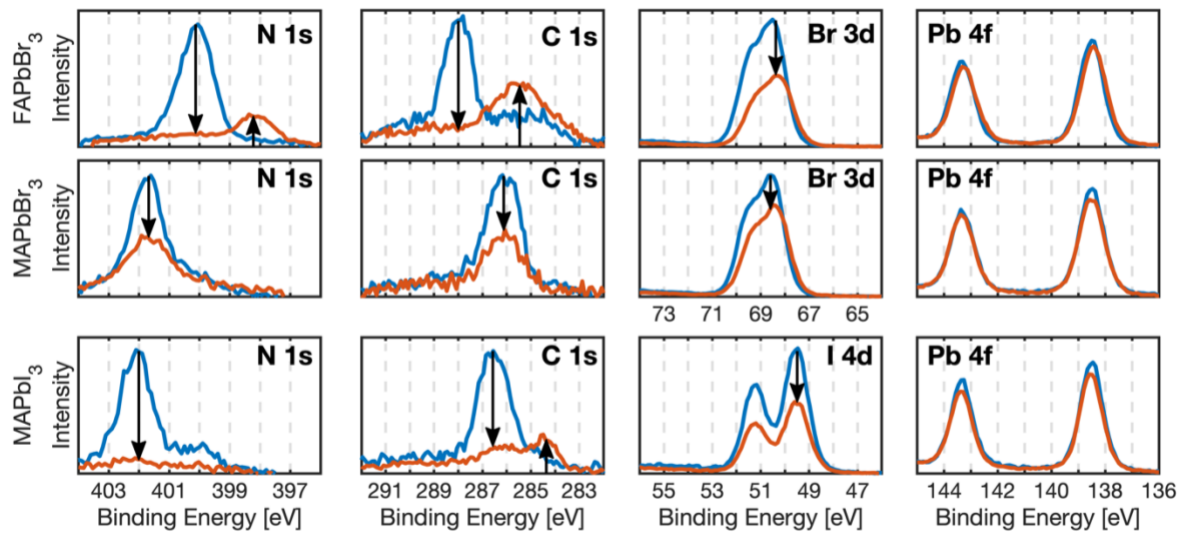
Since single crystals were measured, a homogenous distribution was assumed, and the inelastic mean free path (IMFP) was not considered in the quantitative analysis. The peak area was determined using core level fitting and which was then used to estimate the relative atomic percentages of the different elements at the surface of the crystals. The first measurement of all core levels was considered as the pristine structure and was used as starting point in Figure 2 and 3. Both figures display the ratio between the normalized peak area and starting point measurement, e.g.:  $[\text{area}(x)/\text{area}(\text{Pb}4f)]/[\text{area}(x1)/\text{area}(\text{Pb}4f1)]$ . The initial values were further set according to the pristine perovskite structure (3 halides, 1 A-site cation, 1 nitrogen for MA<sup>+</sup>-based crystals, 2 nitrogen for FA<sup>+</sup>-based crystals, 1 carbon). For the C 1s signal of the newly formed organic species on the FAPbBr<sub>3</sub> crystal surface, only the intensity of the peak fitted at 286.4 eV was considered for the results presented in Figure 3.

The inelastic mean free path (IMFP) was calculated using the TPP-2M method and the results are shown in Table S1.<sup>6</sup> The densities and molecular weights were 4.15 g/cm<sup>3</sup> and 618.97 g/mol for MAPbI<sub>3</sub>, 3.8 g/cm<sup>3</sup> and 238.26 g/mol for MAPbBr<sub>3</sub> and 3.79 g/cm<sup>3</sup> and 491.98 g/mol for FAPbBr<sub>3</sub>.<sup>7</sup> The number of valence electrons was 40 for MAPbI<sub>3</sub> and MAPbBr<sub>3</sub> and 43 for FAPbBr<sub>3</sub>. The kinetic energies were dependent on the crystal composition as well as on the core level and were 461.5 eV for Pb 4f, 531.5 eV for Br 3d, 550.5 eV for I 4d, 313.4 and 198.2 eV for C 1s and N 1s of the MA<sup>+</sup>-based crystals and 312.1 and 200.0 eV for C 1s and N 1s of the FA<sup>+</sup>-based crystals.

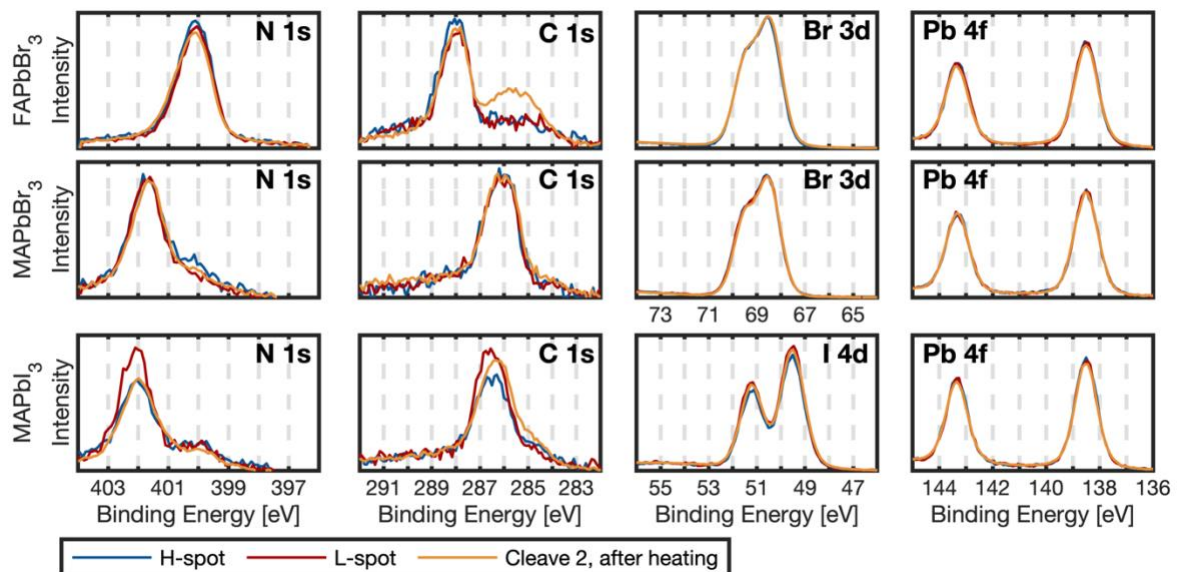
Table S1: Calculation of the inelastic mean free path (IMFP) in dependence of the composition (FAPbBr<sub>3</sub>, MAPbBr<sub>3</sub>, MAPbI<sub>3</sub>) and of the kinetic energy of the corresponding core level using the TPP-2M method at a photoenergy of 600 eV.

Core Level		E <sub>KIN</sub> [eV]	IMFP [nm]		
			FAPbBr <sub>3</sub>	MAPbBr <sub>3</sub>	MAPbI <sub>3</sub>
C 1s	MA <sup>+</sup>	313.4	-	0.93	1.02
	FA <sup>+</sup>	312.1	0.98	-	-
N 1s	MA <sup>+</sup>	198.2	-	0.71	0.76
	FA <sup>+</sup>	200.0	0.74	-	-
Pb 4f		461.5	1.28	1.21	1.32
Br 3d		531.5	1.42	1.33	-
I 4d		550.5	-	-	1.50

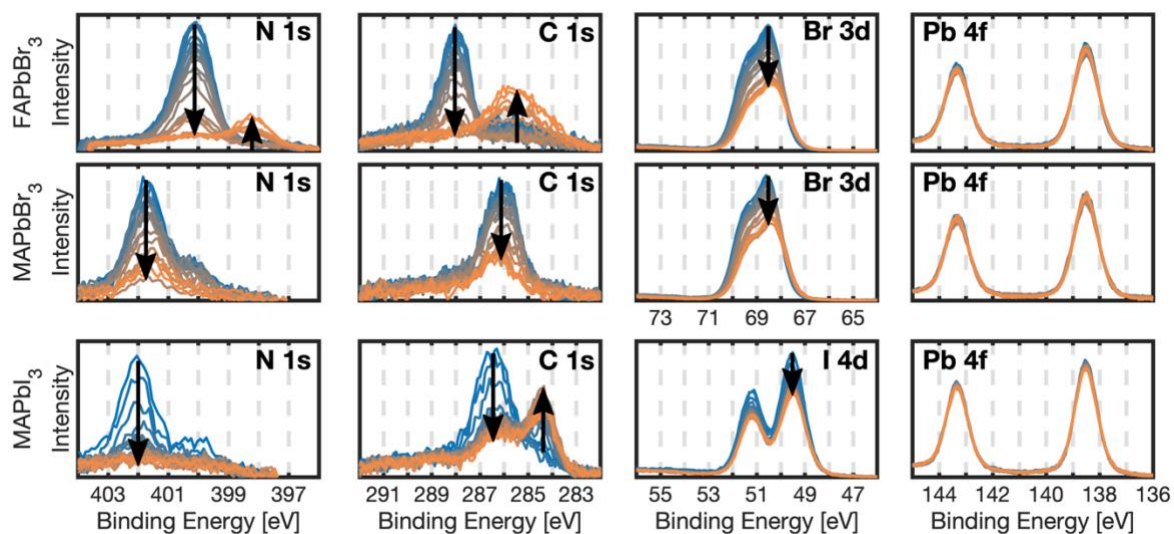
## Figures



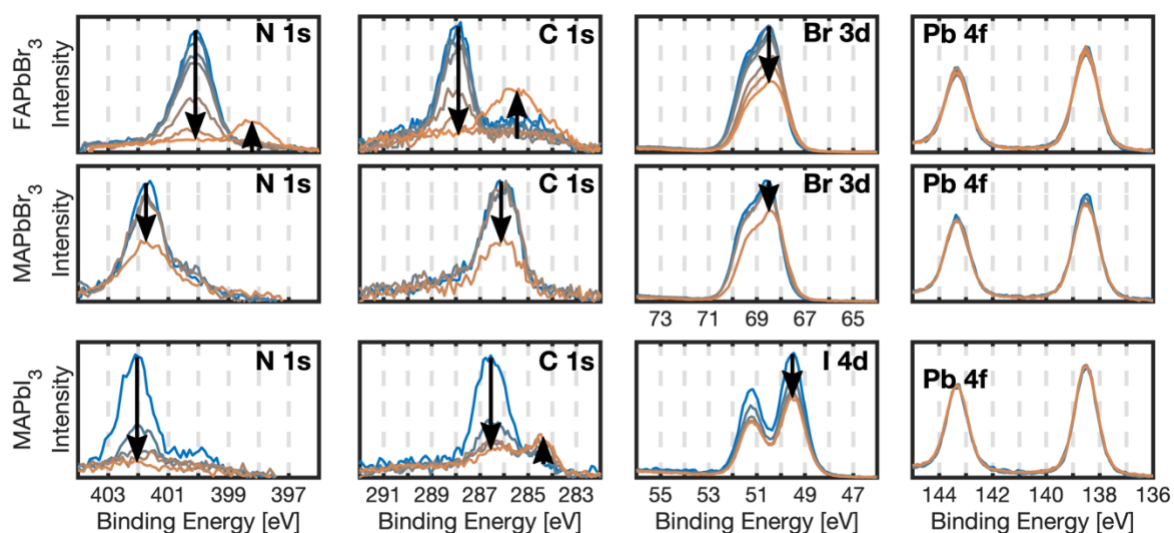
S 2: Core level spectra of the perovskite crystals before heating (T=31.2 °C, blue) and at maximum temperature (T<sub>max</sub>, orange; FAPbBr<sub>3</sub> T<sub>max</sub>=165.9 °C, MAPbBr<sub>3</sub> and MAPbI<sub>3</sub> T<sub>max</sub>=118.4 °C) recorded in the low X-ray exposure spot (L-spot) with a photon energy of 600 eV, normalized to Pb 4f intensity and energy calibrated towards Au 4f<sub>7/2</sub>.



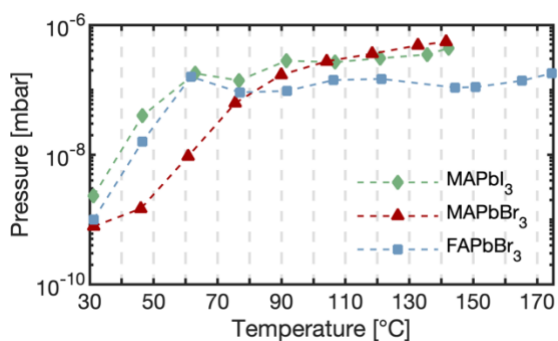
S 3: Core level spectra of N 1s, C 1s, Br 3d / I 4d and Pb 4f of the first measurement before heating at the high X-ray exposure spot (H-spot) and the low X-ray exposure spot (L-spot) as well as of the new surface after cleaving a second time after heating (Cleave 2, after heating) of all crystals using a photon energy of 600 eV. All spectra were intensity normalized towards Pb 4f and energy calibrated towards Au 4f<sub>7/2</sub>. The starting temperature of the sample was 31.22 °C for all crystals. The maximum temperature was 174.5 °C for FAPbBr<sub>3</sub>, 142.3 °C for MAPbI<sub>3</sub>, and 141.5 °C for MAPbBr<sub>3</sub>. The FAPbBr<sub>3</sub> C 1s core level after heating shows additional intensity at lower binding energy which is likely related to insufficient cleaving.



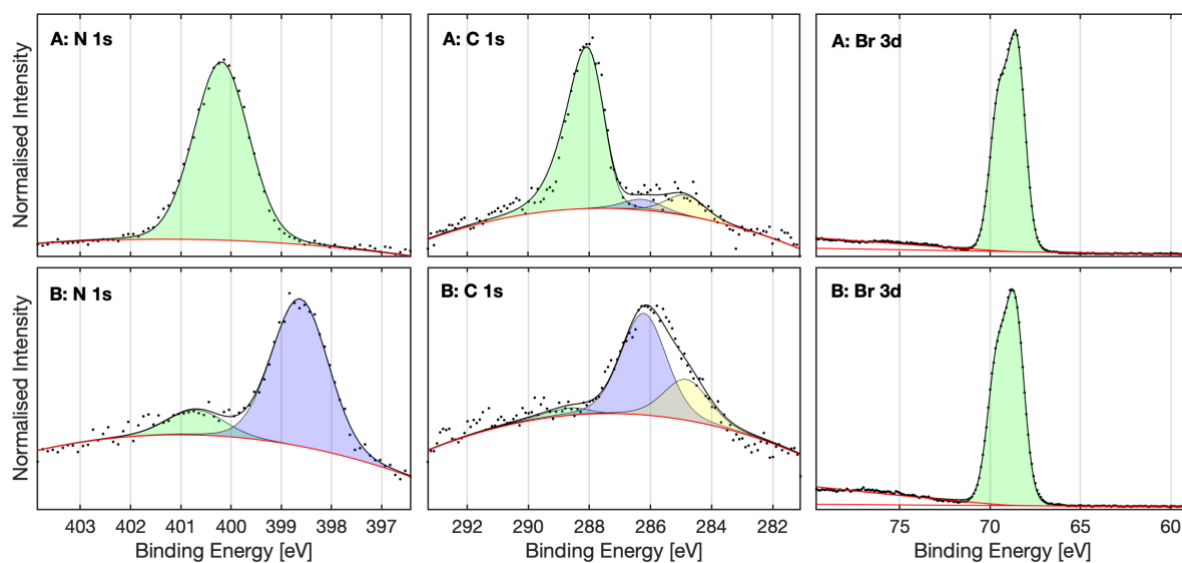
S4: Core level spectra recorded continuously using a photon energy of 600 eV during heating of the single crystals in the H-spot (high X-ray exposure). All spectra were intensity normalized towards Pb 4f and energy calibrated towards Au 4f<sub>7/2</sub>. The starting temperature of the sample was 31.22 °C for all crystals. The maximum temperature was 174.5°C for FAPbBr<sub>3</sub>, 142.3°C for MAPbI<sub>3</sub>, and 141.5°C for MAPbBr<sub>3</sub>.



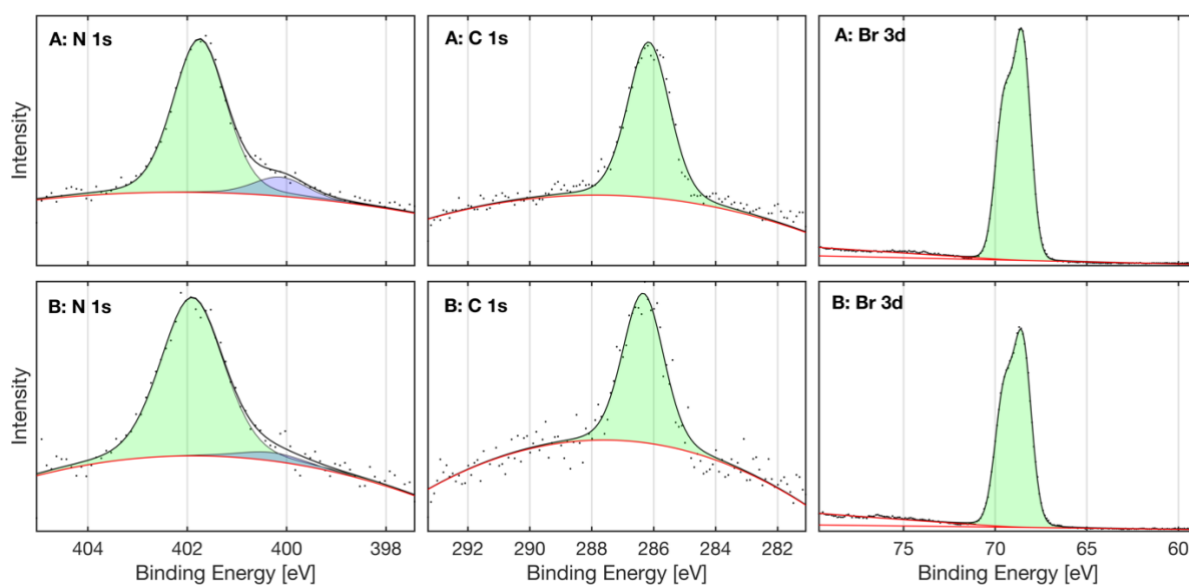
S5: Core level spectra recorded continuously using a photon energy of 600 eV during heating of the single crystals in the L-spot (low X-ray exposure). All spectra were intensity normalized towards Pb 4f and energy calibrated towards Au 4f<sub>7/2</sub>. The starting temperature of the sample was 31.22 °C for all crystals. The maximum temperature was 174.5°C for FAPbBr<sub>3</sub>, 142.3°C for MAPbI<sub>3</sub>, and 141.5°C for MAPbBr<sub>3</sub>.



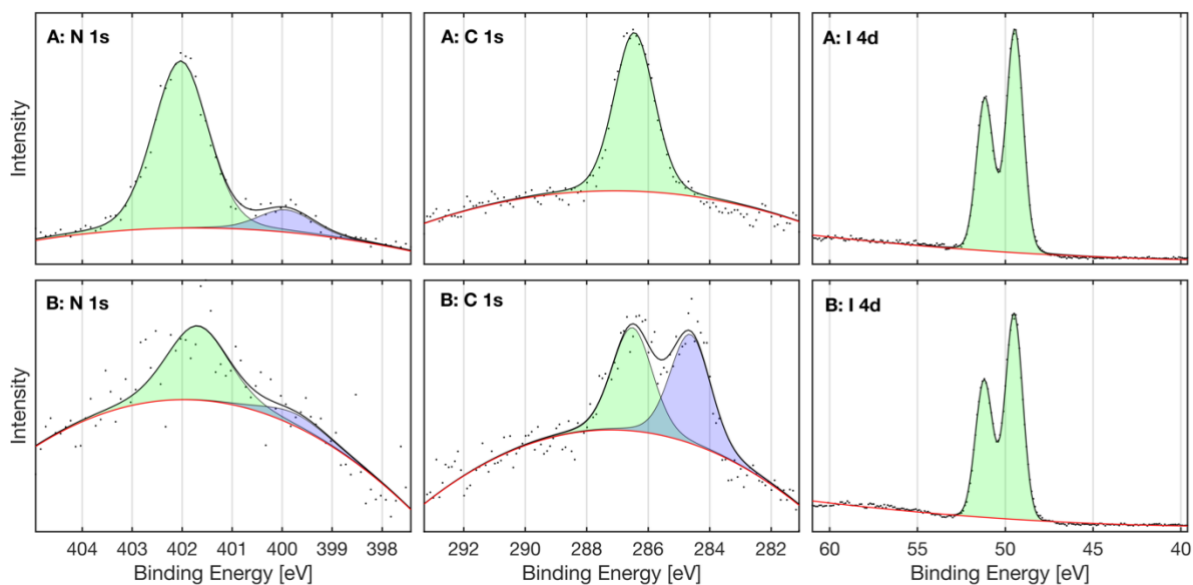
S6: Pressure development in the measurement chamber during the heating experiment. The starting temperature of the sample was 31.22 °C, the maximum temperature was between 141.5 and 174.5 °C, depending on the crystal. The pressure was measured using a Pfeiffer full range pressure gauge (type Bayard Alpert).



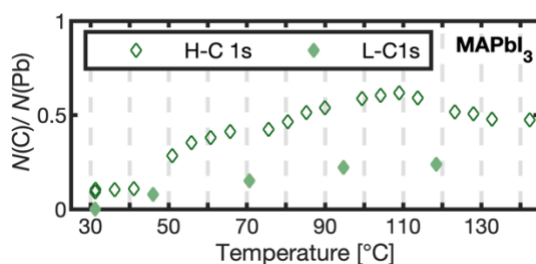
S 7: FAPbBr<sub>3</sub> core level spectra of N 1s, C 1s and Br 3d recorded at a photon energy of 600 eV and fitted before heating (A) and at maximum sample temperature of 174.5 °C (B). The fits of the perovskite peaks are shown in green, whereas the non-perovskite fits are depicted in purple or yellow. The purple fit is correlated to the proposed new species, while the yellow fit is considered to be adventitious carbon.



S 8: MAPbBr<sub>3</sub> core level spectra of N 1s, C 1s and Br 3d recorded at a photon energy of 600 eV and fitted before heating (A) and at maximum sample temperature of 141.5 °C (B). The fits of the perovskite peaks are shown in green, whereas the non-perovskite fits are depicted in purple.



S 9: MAPbI<sub>3</sub> core level spectra of N 1s, C 1s and Br 3d recorded at a photon energy of 600 eV and fitted before heating (A) and at maximum sample temperature of 142.3 °C (B). The fits of the perovskite peaks are shown in green, whereas the non-perovskite fits are depicted in purple.



S 10: Core level intensity evolution as a function of temperature shown as number of carbon atoms N(C) per lead atom N(Pb) forming for high (H-C 1s) and low (L-C 1s) X-ray exposure for MAPbI<sub>3</sub>.

## Formation of a new species in the C 1s spectrum for MAPbI<sub>3</sub>

A new species at 284.6 eV was observed in the C 1s spectrum of MAPbI<sub>3</sub> (Figure S2). The intensity of this new carbon species is significantly higher at the H-spot than at the L-spot (Figure S10), which indicates X-ray dose dependent contributions. Since no nitrogen species is forming and taking the increasing pressure in the measurement chamber into consideration (Figure S6), the formation of a new organic compound from the perovskite is unlikely. Contamination with adventitious carbon in PES measurements is commonly known and usually attributed either to accumulation of carbon on the surface from the measurement chamber itself or to air-contamination.<sup>8,9</sup> Here, a temperature-dependent ad- and desorption of adventitious carbon on the sample plate and the crystal surface is likely observed. Except for the C 1s core level of MAPbI<sub>3</sub>, none of the changes in the other core level spectra of all three compounds depend on X-ray exposure and we therefore do not observe X-ray induced damage of the perovskite.

## References

- 1 T. Leitner, A. Born, I. Bidermane, R. Ovsyannikov, F. O. L. Johansson, Y. Sassa, A. Föhlisch, A. Lindblad, F. O. Schumann, S. Svensson and N. Mårtensson, *J. Electron Spectrosc. Rel. Phenom.*, 2021, **250**, 147075.
- 2 K. Hollmack, R. Ovsyannikov, P. Kuske, R. Müller, A. Schällicke, M. Scheer, M. Gorgoi, D. Kühn, T. Leitner, S. Svensson, N. Mårtensson and A. Föhlisch, *Nat. Commun.*, 2014, **5**, 4010.
- 3 T. Ida, M. Ando and H. Toraya, *J. Appl. Crystallogr.*, 2000, **33**, 1311–1316.
- 4 D. A. Shirley, *Phys. Rev. B*, 1972, **5**, 4709–4714.
- 5 A. García-Fernández, S. Svanström, C. M. Sterling, A. Gangan, A. Erbing, C. Kamal, T. Sloboda, B. Kammlander, G. J. Man, H. Rensmo, M. Odelius and U. B. Cappel, *Small*, 2022, **18**, 2106450.
- 6 C. J. Powell, *J. Vac. Sci. Techn. A*, 2020, **38**, 023209.
- 7 Y. Rakita, S. R. Cohen, N. K. Kedem, G. Hodes and D. Cahen, *MRS Commun.*, 2015, **5**, 623–629.
- 8 H. Piao and N. S. McIntyre, *Surf Interface Anal.*, 2002, **33**, 591–594.
- 9 E. Desimoni, G. I. Casella, A. M. Salvi, T. R. I. Cataldi and A. Morone, *Carbon N Y*, 1992, **30**, 527–531.